Maxwell Nano-Fluid Flow, Heat and Mass Transfer Effects in a Vertical Wavy Channel with Multiple Slip

Khaja Hassan[1], R. VijayaKumar[2,*] and G. Srinivas[3]

[1]*Department of Mathematics, Guru Nanak Institute of Technology, Khanapur, Ibrahimpatnam, Hyderabad, 501506, Telangana State, India.*
[2]*Mathematics Section, Faculty of Engineering and Technology, Annamalai University, Annamalainagar, Chidambaram-608002,*

Tamilnadu, India.

Department of Mathematics, Periyar Government Arts College, Cuddalore- 608002, Tamilnadu, India.

[3]*Department of Mathematics, Guru Nanak Institute of Technology, Khanapur, Ibrahimpatnam, Hyderabad, 501506, Telangana State, India.*

Corresponding author Email address: rathirath_viji@yahoo.co.in

ABSTRACT :

The current research is the study of the heat and mass transfer via vertical wavy channel due to numerous industrial applications as many fluid carriers are not uniform due to the circumstances or due to the maintenance. The dented and wavy fluid carriers are more frequent in industrial applications. Maxwell nano-fluid is considered as medium in this study. Thermal slip and diffusion slip Effects have been investigated. The Mathematically modelled governing equations are Coupled partial differential equations. The solution of this system of equations is interesting. These are solved by using Finite Element Method with the help of Mathematica computer software. The significant numerical results are derived and are provided in the form of graphs for all the non-dimensional parameters under consideration. The detailed discussion is also presented. Both the Nusselt Number and Sherwood Number values have been computed for all the variations of all dimensionless parameters. It is found that the thermal slip retards the rate of heat transfer significantly on the source wall but enhances on the sink wall. The Maxwell parameter enhances the heat transfer rate on both walls notably.

Keywords: Maxwell Nano-fluid, Wavy channel, Nanofluid, Thermal slip, Diffusion Slip, FEM.

Nomenclature:

α	Constant
B	Volumetric expansion coefficient
C_p	Specific heat capacity of nanoparticle material

d	Distance between the two wavy walls divided in half
D_B	Brownian diffusion coefficient
g	Acceleration at the right wall of the channel
G_C	Molecular Grashvof number
G_r	Thermal Grashvof number
L_n	Nanofluid Lewis number
M	Magnetic field parameter
Nb	Brownian Motion parameter
Nt	Thermophoresis parameter
Nu	Rate of heat transfer coefficient (or) Nusselt number
Pr	Prandtl number
Q	Heat source parameter
S	Dimensionless diffusion
Sh	Rate of mass transfer coefficient (or) Sherwood number
t	Time
t'	Non dimension time
T	Fluid temperature (K)
u, v	Velocity components in x and y axes respectively (m/s)
U	The Velocity of the mentioned fluid in horizontal direction
V	The Velocity of the mentioned fluid in vertical direction

x, y	Measuring along the stretching sheet

Greek symbols:

$\propto$	Thermal Diffusivity
$\propto_{nf}$	Thermal Diffusivity of nanofluid
β	Thermal slip
γ	Thermal relaxation time parameter
δ	Diffusion slip
ε	Wave amplitude
θ	Dimensionelss temperature (K)
K_0	Maxwell fluid parameter
k_f	Thermal conducting of fluid
k_{nf}	Thermal conducting of nanofluid
λ	Non dimensional wave number
μ	Viscosity
μ_f	Fluid viscosity
μ_{nf}	Nanofluid Viscosity
ν	Kinematic viscosity (m^2/s)
ν_{nf}	Kinematic viscosity of the nanofluid
ρ	Density
ρ_f	Density of the nanofluid
σ	Electrical conductivity
ϕ	Dimensionless nanofluid concentration (mol/m^3)
ψ	Stream function
ω	non dimensional due to gravity

1. <u>INTRODUCTION:</u>

The use of free convective flows over wavy walls in various engineering and industrial applications has gained attention in recent years. This includes applications such as drying agricultural products, ventilating for heating buildings, cooling electronic components, and enhancing mass transfer in medical procedures. Wavy walls are commonly employed to control the flow velocity and heat transfer in cooling and heating systems. Heat conduction occurs when there is a temperature gradient in a solid, and it involves the transfer of energy from higher energetic molecules to lesser energetic ones through molecular collisions. The process of heat conduction relies on the temperature and properties of the materials involved. Maxwell nano-fluids, which facilitate the movement of heat and mass, find utility in diverse fields such as production processes, fiber melting, agriculture, chemical reactions, and industrial applications.

L.Y. Zhang a et.al.[1] reported that wavy channel expedites and fasten the heat transfer rate. Igor V. Miroshnichenko et.al. [2] examined the convection of micropolar fluid in a horizontal wavy channel under local heating and noticed that the Rayleigh number symbolizes the dominance of natural convection regime with the production of recirculation along the top wall. Abdullah Dawar, Zahir Shah [3] was studied the causes of heat sink, thermal radiation on Eyringpowell fluid past an unsteady periodic porous stretching surface numerically. S.E. Ghasemi et.al [5] indicated that the rise in Brownian motion enhances the temperature, stressing the importance of nano fluid. Several researchers investigated how nanofluid will affect diverse applications [6-11]. Nadeem et al. [12] examined the intensity move of Maxwell base nanomaterial fluid stream with MHD across a moving vertical plane utilizing a moving vertical plane. The consolidated responses of emanation and MHD on flexible sticky fluid course

131

through a pervious plate were researched by Hussian et al. [13] in their review. Researchers examined the responses of an attractive field and an intensity source on the way of behaving of Upper-sentenced Maxwell fluid in permeable channels to get a superior comprehension of the fluid's way of behaving [14]. Sravanthi and Gorla [15] used the homotopy examination strategy to research the responses of intensity source/sink and compound response on MHD Maxwell nanofluid stream during a convectively warmed dramatically extended sheet in their MHD Maxwell nanofluid stream study. Utilizing a dramatically rising plane region, Farooq et al. [16] examined the MHD stream of a Maxwell liquid including nanoparticles. As per Imran et al. [17], a MHD summed up Maxwell liquid streamed in a limit layer over an endless vertical plane with dramatically sped up slip and Newtonian warming, as found in a limit layer. A portion of the exploration works ([18]-[30]) concentrated on the qualities of nanofluid streams in presence of different fields.

From all the above studies the wavy geometry is more significant in fluid carriers when there is dent or small bend. Keeping this in view, we have investigated the influence of thermal and diffusion slip effects on Maxwell nano fluid flow, heat and mass transfer through the wavy vertical channel.

2. <u>MATHEMATICAL MODELLING:</u>

We took Maxwell nanofluid flow into consideration between the vertical channel's two wavy walls. We thought about fluid flow along an x-axis and thought about a y-axis that was perpendicular to fluid flow. The vertical channel's two side walls are at $y = d + \varepsilon \cos \lambda x$ and $y = -d + \varepsilon \cos(\lambda x + \zeta)$. Buoyancy is the cause of the upward flow. Due to the root cause of temperature differences along the direction of flow and density variation ρ. Consideration is given to the thermal slip and diffusion slip on the heated wall.. The schematic diagram is shown below:

132
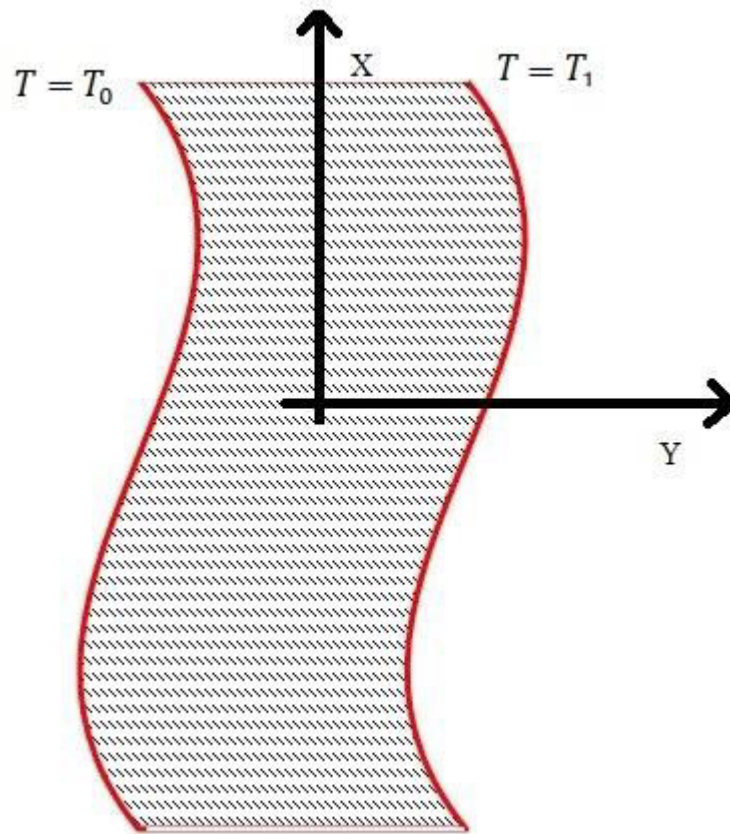
$$y = -d + \epsilon \cos(\lambda x) \qquad y = d + \epsilon \cos(\lambda x + \zeta)$$

We suppose that length of the wave of a vertical wavy wall is equivalent to reciprocal of λ. A fluid streaming is believed that to follow the bounessq approximation. With these assumptions the governing equations are as given below:

Continuity equation is

$$\frac{\partial u}{\partial x} + \frac{\partial v}{\partial y} = 0 \tag{1}$$

Momentum Equation is

$$\left(\frac{\partial u}{\partial t}\right) + u\left(\frac{\partial u}{\partial x}\right) + v\left(\frac{\partial u}{\partial y}\right) = v_{nf}\left(\frac{\partial^2 u}{\partial x^2} + \frac{\partial^2 u}{\partial y^2}\right) - \left(\frac{\sigma B_o^2}{\rho_{nf}}\right)u + \left(\frac{gB_T(T-T_0)}{\rho_{nf}}\right) + \left(\frac{gB_c(\phi-\phi_0)}{\rho_{nf}}\right) - k_o\left(u^2\frac{\partial^2 u}{\partial x^2} + v^2\frac{\partial^2 u}{\partial y^2} + 2uv\frac{\partial^2 u}{\partial x \partial y}\right) \tag{2}$$

$$\left(\frac{\partial v}{\partial t}\right) + u\left(\frac{\partial v}{\partial x}\right) + v\left(\frac{\partial v}{\partial y}\right) = v_{nf}\left(\frac{\partial^2 v}{\partial x^2} + \frac{\partial^2 v}{\partial y^2}\right) - \left(\frac{\sigma B_o^2}{\rho_{nf}}\right)v - k_o\left(u^2\frac{\partial^2 u}{\partial x^2} + v^2\frac{\partial^2 u}{\partial y^2} + 2uv\frac{\partial^2 u}{\partial x \partial y}\right) \tag{3}$$

$$\left(\frac{\partial T}{\partial t}\right)+u\left(\frac{\partial T}{\partial x}\right)+v\left(\frac{\partial T}{\partial y}\right)=\alpha_{nf}\left(\frac{\partial^2 T}{\partial x^2}+\frac{\partial^2 T}{\partial y^2}\right)+\tau\left\{D_B\left(\frac{\partial \phi}{\partial y}\right)\left(\frac{\partial T}{\partial y}\right)+\left(\frac{\partial \phi}{\partial x}\right)\left(\frac{\partial T}{\partial x}\right)\right\}+\left\{\frac{D_T}{Ts}\left(\frac{\partial T}{\partial x}\right)^2+\left(\frac{\partial T}{\partial y^2}\right)^2\right\} \quad (4)$$

$$\left(\frac{\partial \phi}{\partial t}\right)+u\left(\frac{\partial \phi}{\partial x}\right)+v\left(\frac{\partial \phi}{\partial y}\right)=D_s\left(\frac{\partial^2 \phi}{\partial x^2}+\frac{\partial^2 \phi}{\partial y^2}\right)+\frac{D_T}{Tc}\left(\frac{\partial^2 T}{\partial x^2}+\frac{\partial^2 T}{\partial y^2}\right) \quad (5)$$

The bondary conditions are :

$$u=0, v=0, T=T_1+\beta\frac{\partial T}{\partial y}, \phi=\phi_1+\delta\frac{\partial \phi}{\partial y} \quad at \ t\ge 0, \forall x, \ y=-d+\varepsilon Cos(\lambda x+t)$$

$$u=0, v=0, T=T_0, \ \phi=\phi_0 \quad at \ t\ge 0, \forall x, \ y=d+\varepsilon Cos(\lambda x+t)$$

All the equations from (1) to (5) are created dimensionless using the following forms:

$$X=\frac{x}{d}, Y=\frac{y}{d}, U=\frac{ud}{x}, V=\frac{vd}{x}, \lambda'=\lambda d, t'=\frac{tv}{t^2}, \theta=\frac{T-T_0}{T_1-T_0}, s=\frac{\phi-\phi_0}{\phi_1-\phi_0}.$$

All the above equations (1) to (5) becomes

$$\left(\frac{\partial U}{\partial t}\right)+U\left(\frac{\partial U}{\partial X}\right)+V\left(\frac{\partial U}{\partial Y}\right)=\frac{v_{nf}}{v_f}\left(\frac{\partial^2 U}{\partial X^2}+\frac{\partial^2 U}{\partial Y^2}\right)-MU+Gr\theta+Gc\,C-\gamma\left(U^2\frac{\partial^2 U}{\partial X^2}+V^2\frac{\partial^2 V}{\partial Y^2}+2UV\frac{\partial^2 U}{\partial X\partial Y}\right) \quad (6)$$

$$\left(\frac{\partial V}{\partial t}\right)+U\left(\frac{\partial V}{\partial X}\right)+V\left(\frac{\partial V}{\partial Y}\right)=\frac{v_{nf}}{v_f}\left(\frac{\partial^2 V}{\partial X^2}+\frac{\partial^2 V}{\partial Y^2}\right)-M\,V-\gamma\left(U^2\frac{\partial^2 U}{\partial X^2}+V^2\frac{\partial^2 V}{\partial Y^2}+2UV\frac{\partial^2 U}{\partial X\partial Y}\right) \quad (7)$$

$$\left(\frac{\partial \theta}{\partial t}\right)+U\left(\frac{\partial \theta}{\partial X}\right)+V\left(\frac{\partial \theta}{\partial Y}\right)=\frac{1}{Pr}\frac{\alpha_{nf}}{\alpha_f}\left(\frac{\partial^2 \theta}{\partial X^2}+\frac{\partial^2 \theta}{\partial Y^2}\right)+N_b\left(\left(\frac{\partial S}{\partial Y}\right)\left(\frac{\partial \theta}{\partial Y}\right)+\left(\frac{\partial S}{\partial X}\right)\left(\frac{\partial \theta}{\partial X}\right)\right)+N_t\left(\left(\frac{\partial \theta}{\partial X}\right)^2+\left(\frac{\partial \theta}{\partial Y}\right)^2\right) \quad (8)$$

$$\left(\frac{\partial S}{\partial t}\right)+U\left(\frac{\partial S}{\partial X}\right)+V\left(\frac{\partial S}{\partial Y}\right)=Nb\,Ln\left(\frac{\partial^2 S}{\partial X^2}+\frac{\partial^2 S}{\partial Y^2}\right)-Nt\left(\left(\frac{\partial^2 \theta}{\partial X^2}\right)+\left(\frac{\partial^2 \theta}{\partial Y^2}\right)\right) \quad (9)$$

The dimensionless boundary conditions are:

$$U=0, V=0, \theta=1+\beta\theta', s=1+\delta s' \quad at \ t'\ge 0, \forall X, \ Y=-1+\varepsilon Cos(\lambda x+t)$$
$$U=0, V=0, \theta=0, s=0 \quad at \ t'\ge 0, \forall X, \ Y=1+\varepsilon Cos(\lambda x+t)$$

Where

$$Gr=\frac{g\beta_T(T_1-T_0)d^3}{v_{nf}^2}, \ Gc=\frac{g\beta_C(\phi_1-\phi_0)d^3}{v_{nf}^2}, Pr=\frac{v_{nf}}{\alpha_{nf}}, \gamma=k_0 d, Nb=\frac{(\rho c_p)_{nf}D_B(\phi_1-\phi_0)}{k}, Nt=\frac{(\rho c_p)_{nf}D_T(T_1-T_0)}{kT_0}, Ln=\frac{v_{nf}}{D_B}, M=\frac{\sigma B_0^2}{\rho_{nf}d}$$

$$\rho_{nf}=(1-\psi)\rho_f+\psi\rho_s, \alpha_{nf}=\frac{k_{nf}}{(\rho c_p)_{nf}}, (\rho c_p)_{nf}=(1-\psi)(\rho c_p)_f+\psi(\rho c_p)_s$$

$$\frac{\mu_{nf}}{\mu_f}=1+2.5\psi, \ \frac{k_{nf}}{k_f}=\frac{(k_s+2k_f)-2\psi(k_f-k_s)}{(k_s+2k_f)+2\psi(k_f-k_s)}$$

The rate of heat transfer (Nusselt Number) is calculated on both wavy walls using the following formulae

$$Nu1=\left(\frac{\partial \theta}{\partial Y}\right) at \ -1+\varepsilon Cos(\lambda x+t)$$

134

$$Nu2 = \left(\frac{\partial \theta}{\partial Y}\right) at \ 1 + \varepsilon Cos(\lambda x + t)$$

The rate of mass transfer (Sherwood Number) is calculated on both wavy walls using the following formulae

$$Sh1 = \left(\frac{\partial S}{\partial Y}\right) at \ -1 + \varepsilon Cos(\lambda x + t)$$

$$Sh2 = \left(\frac{\partial S}{\partial Y}\right) at \ 1 + \varepsilon Cos(\lambda x + t)$$

3. Solution of the problem:

All the equations from (6) to (9) are solved using the transformation g(x,y,t)=g(y) $e^{i(ax+st)}$ as given in N. Rudraiah et.al [2011]. Finite Element Method is the one that has been used to solve the resultant equations by using Mathematica software. The iterations are applied until the accuracy of 10^{-3} has achieved. The constants are remain unchanged throught the entire computation process are M=0.5, Gr=5, Gc=5, γ =0.5, β=0.5, λ =0.5, δ=0.5, ε=0.02, Nb=0.8, Nt=0.8, Ln=0.8, Pr= 0.71, ψ =0.05.

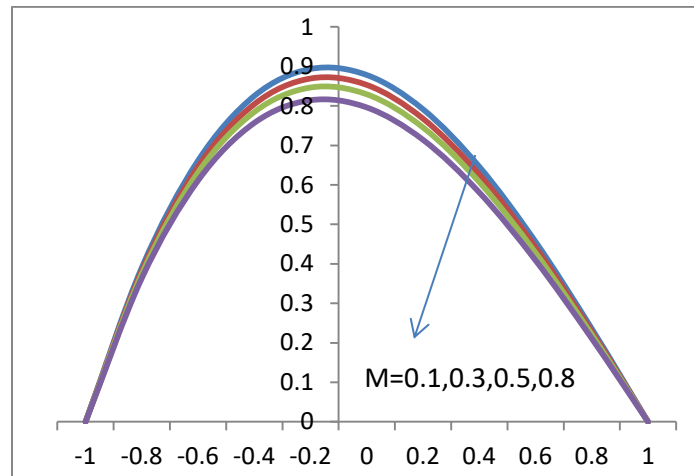## 4. Discussion of Results:

Fig.1 Variation of U with M
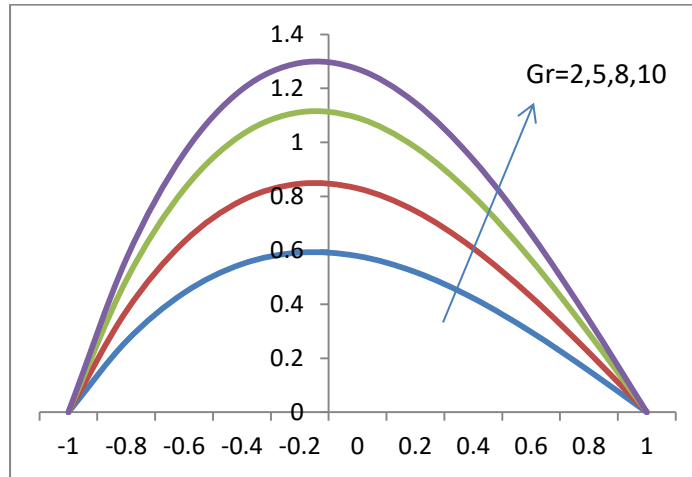
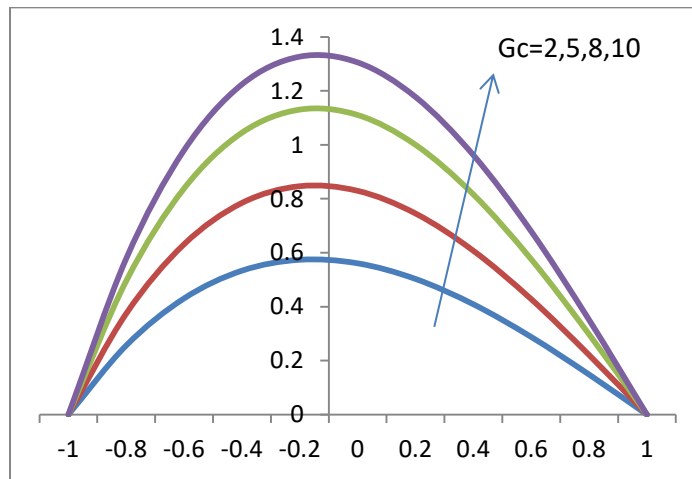Fig. 2 Variation of U with Gr

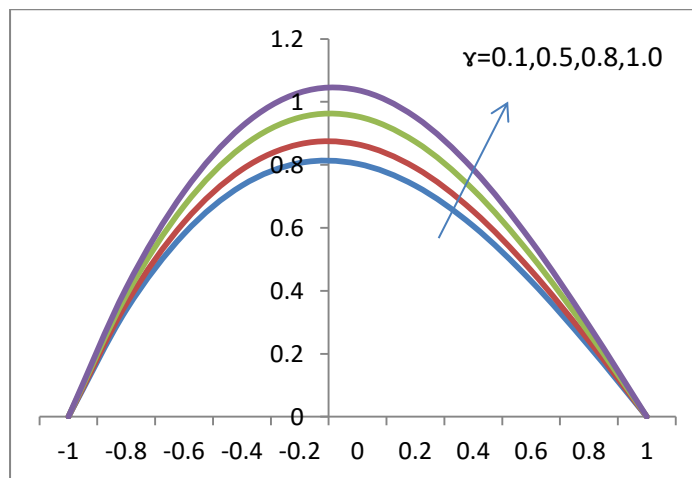
Fig. 3 Variation of U with Gc
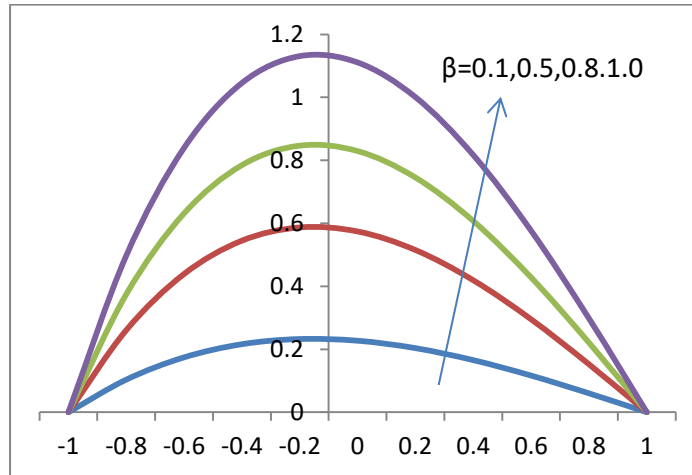

Fig. 4 Variation of U with ɤ
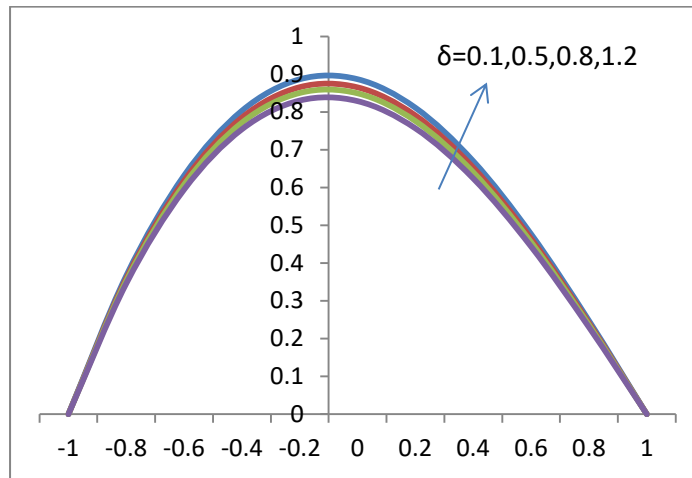
Fig. 5 Variation of U with β

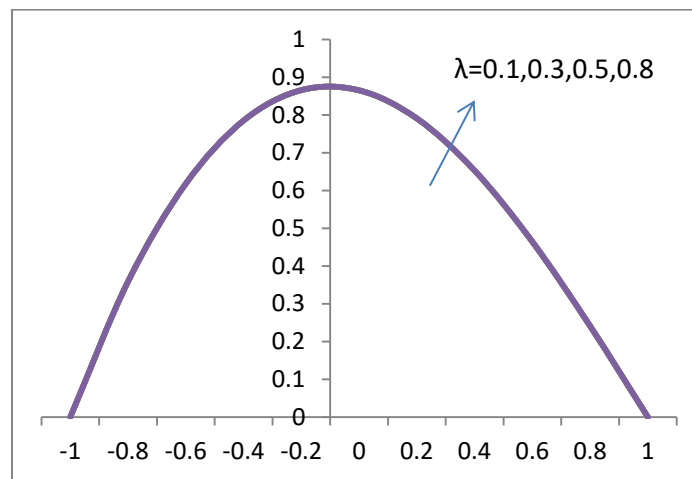Fig. 6 Variation of U with δ
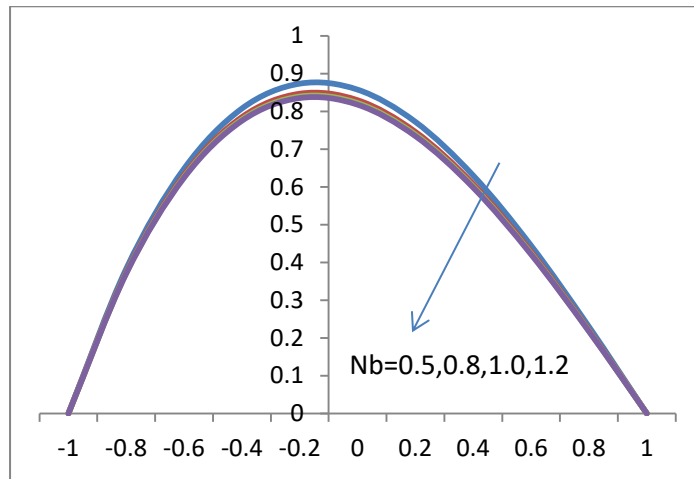

Fig. 7 Variation of U with λ

137

Fig. 8 Variation of U with Nb

Fig. 9 Variation of U with Nt

Fig.10 Variation of U with Ln

Fig.11 Variation of V with M

Fig. 12 Variation of V with ɤ

Fig. 13 Variation of θ with M

ɤ=0.1,0.5,0.8,1.0

Fig. 14 Variation of θ with ɤ

β=0.8,0.5,0.3,0.1

Fig. 15 Variation of θ with β

Fig. 16 Variation of θ with λ

Fig. 17 Variation of θ with Nb

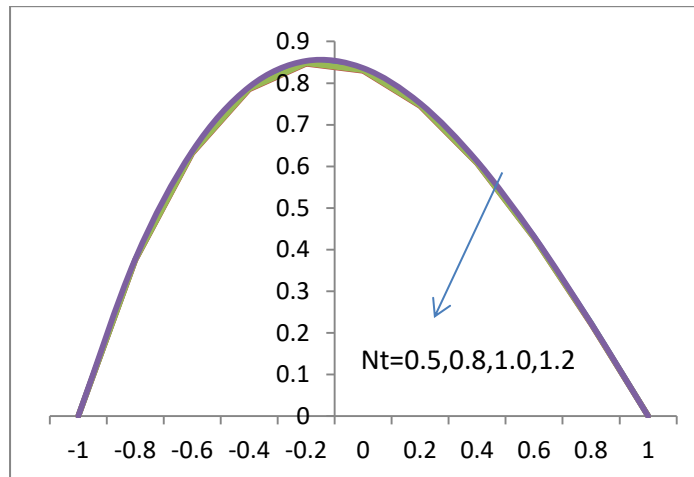Fig. 18 Variation of θ with Nt

141

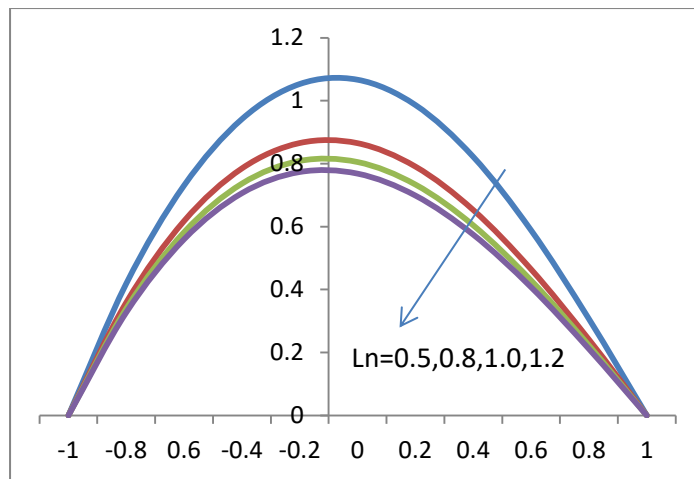Fig. 19 Variation of S with M

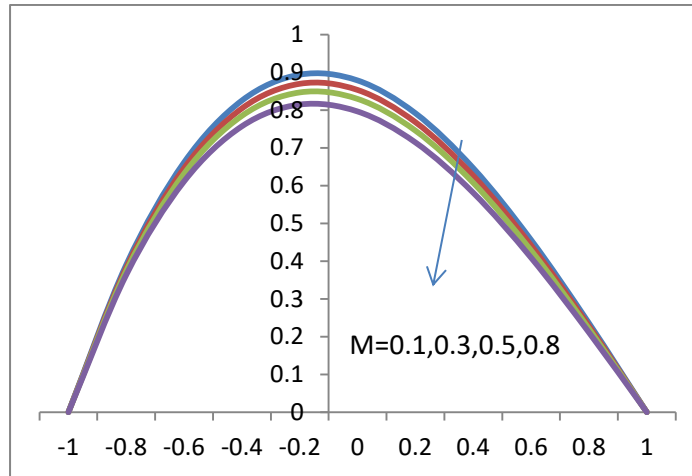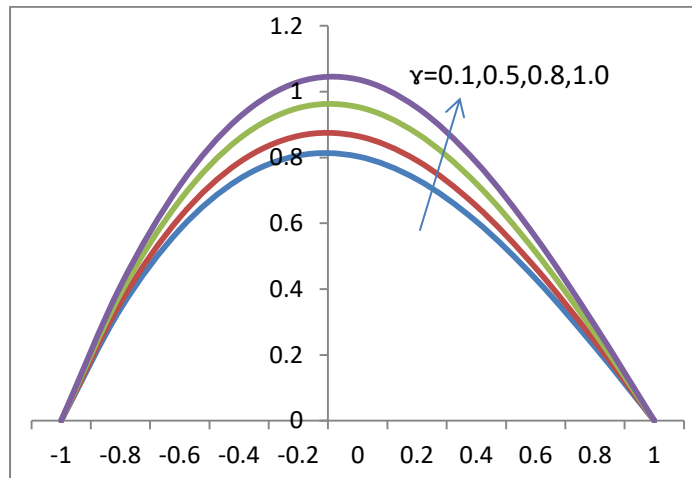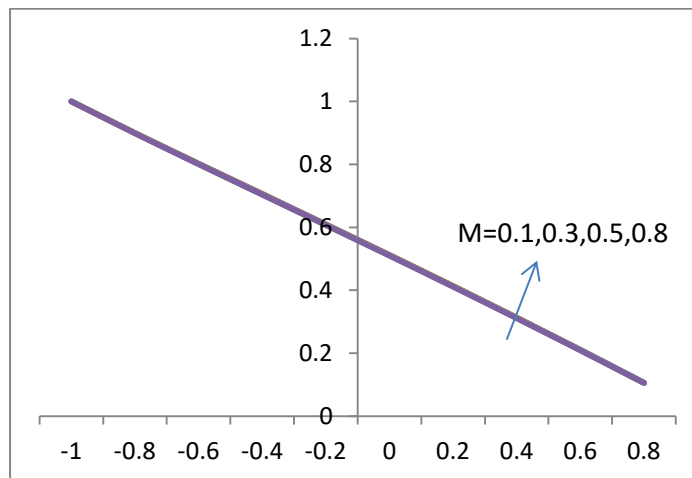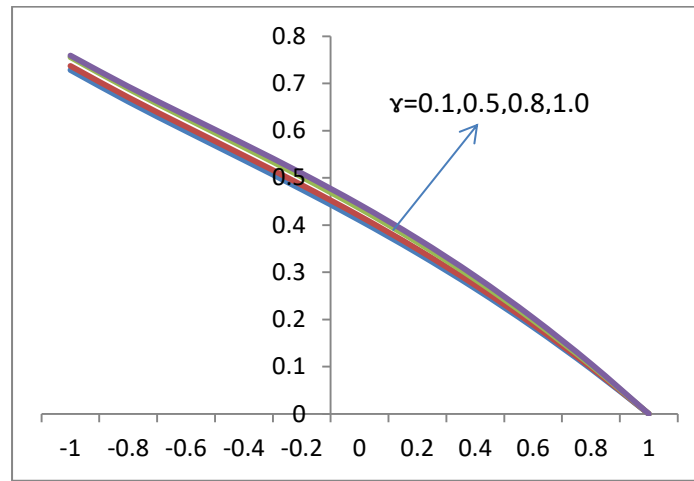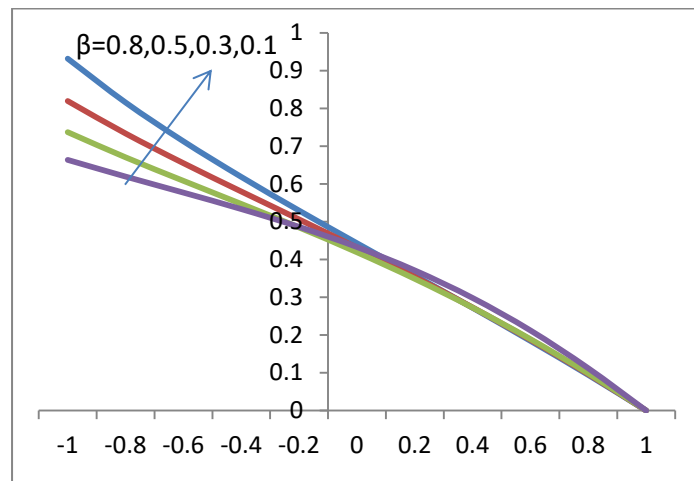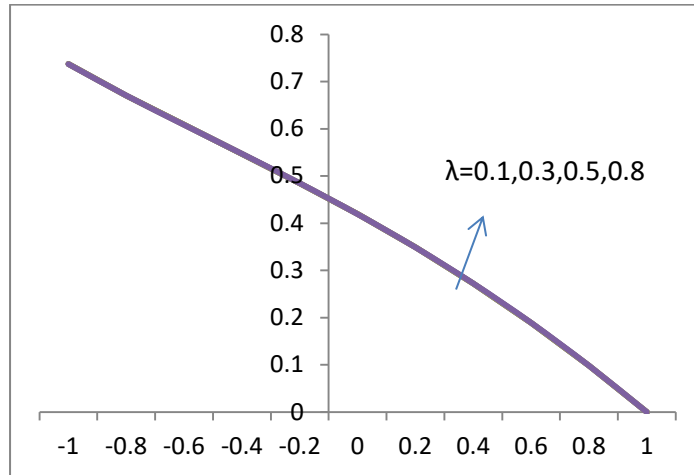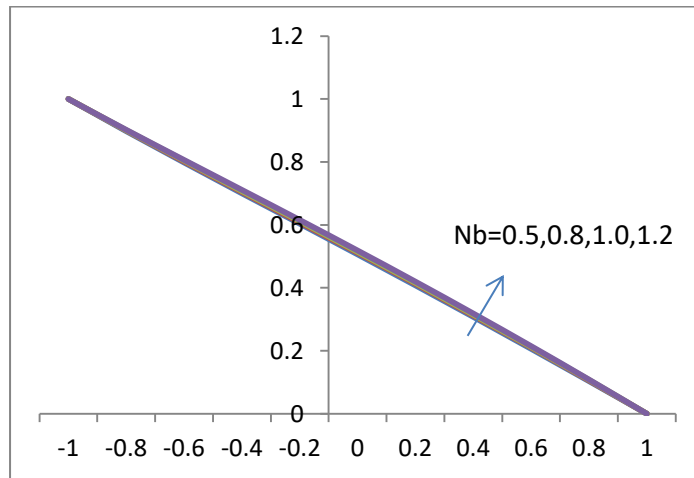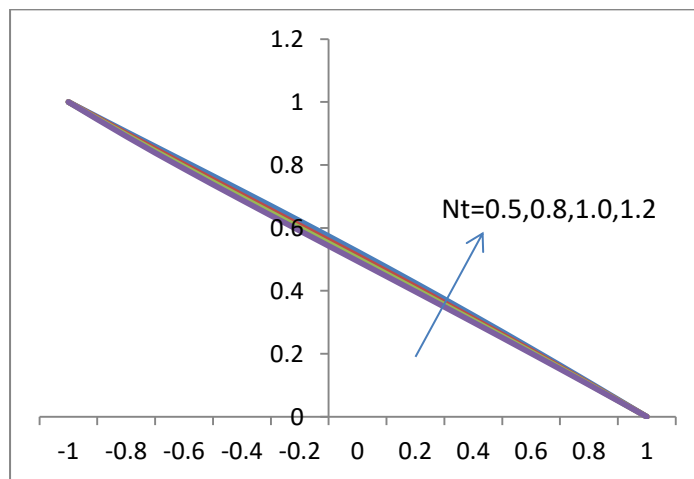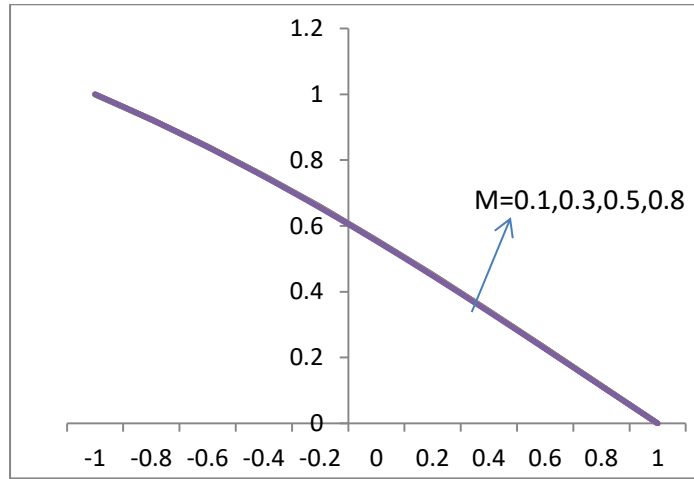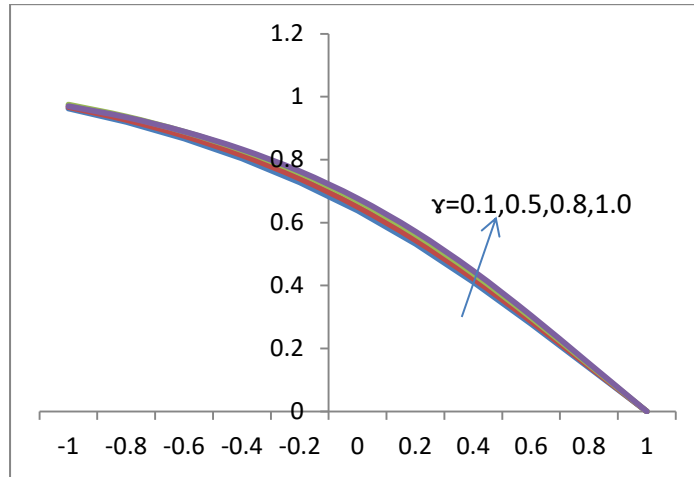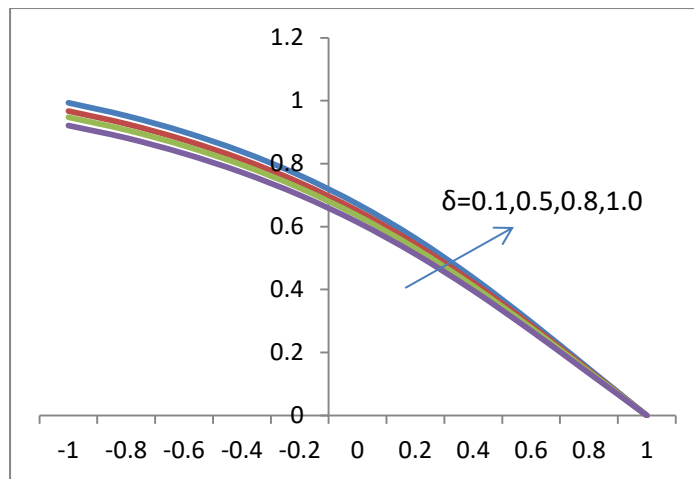Fig. 20 Variation of S with ɤ

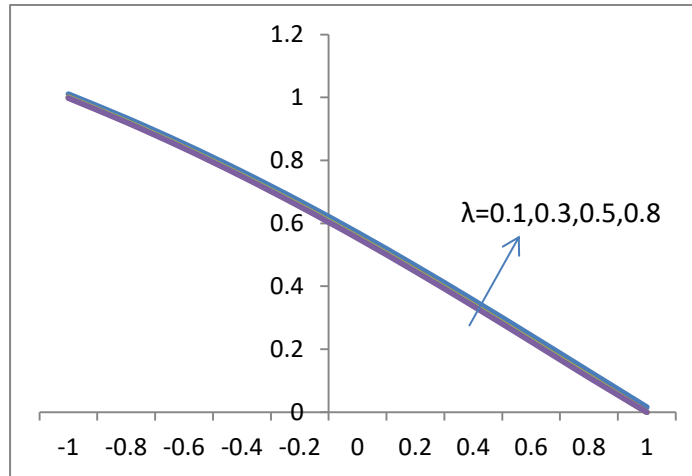Fig. 21 Variation of S with δ

Fig. 22 Variation of S with λ
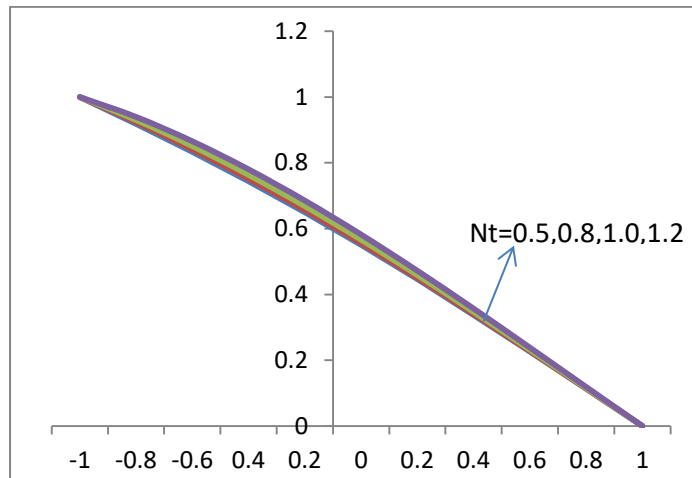
Fig. 23 Variation of S with Nt

143
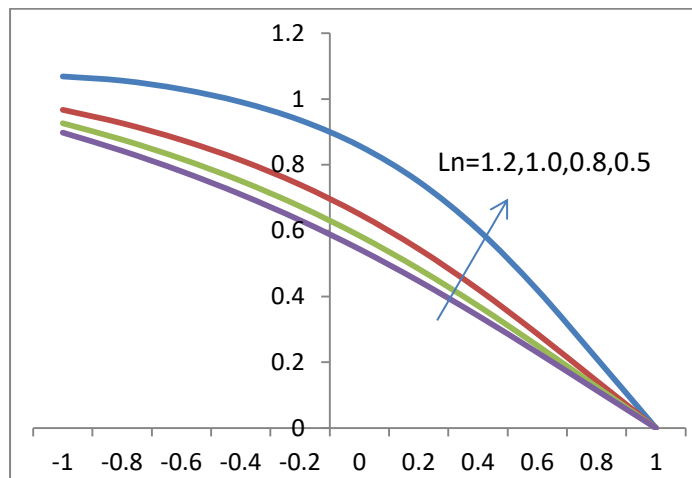
Fig. 24 Variation of S with Ln
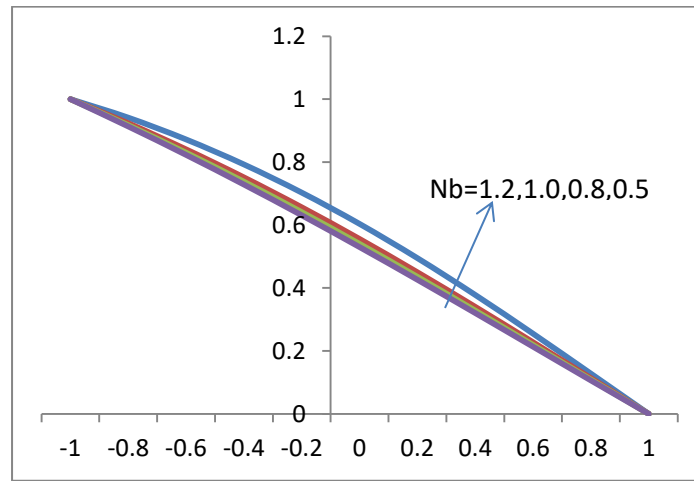
Fig. 25 Variation of S with Nb

The typical cross section of wavy channel is taken into consideration for numerical calculation. The results are displayed graphically from Fig.1 to Fig.25 for all governing parameters. The dimensionless numbers are kept constant as M= 0.5, Gr=5, Gc=5, γ =0.5, β =0.5, λ =0.5, δ=0.5, ε=0.02, Nb=0.8, Nt=0.8, Ln=0.8, Pr= 0.7 throughout the study except for the particular variation. The Fig.1 to Fig.10 illustrate the changes in velocity (u) across all dimensionless numbers. Fig.1 displays the variation of u with the magnetic field (M). The velocity is found maximum in the mid region and further it is observed that the Lorentz force retards the velocity all through the channel. Fig.2 Exhibits the differences of u with thermal Grashof Number (Gr). It is observed that the thermal buoyancy force dominates the viscous force in enhancing the velocity u throughout the channel. Fig.3 Demonstrate how u varies with solutal Grashof Number (Gc). Solutal buoyancy force enhances the velocity u like the thermal buoyancy force. Fig.4 Illustrate how u changes with respect to Maxwell parameter (γ). The significance of Maxwell fluid is clear in this figure and it is observed that the Maxwell fluid enhances the velocity u. Fig.5 shows the variation of u with Thermal slip (β). The velocity u enhances with the thermal slip and the velocity is maximum in the mid region. Fig.6 displays the velocity (u) with diffusion slip (δ). The increase in diffusion slip enhances the velocity slightly unlike the thermal slip. Fig.7 Presents how the wave fequency (λ) effects the variation of velocity u. The velocity (u) enhances slightly with increase in wave frequency parameter (λ). Fig.8 shows the velocity profile of u as influenced by the Brownian motion parameter (Nb). As the Brownian motion increases the fluid particle distribution is random so the velocity reduces with Nb slightly. Fig.9 demonstrate how the thermophoresis parameter (Nt) affects the variation of velocity u. The increase in Thermophoresis parameter reduces the velocity throughout the region. Fig.10 illustrate how Ln affects the variation of velocity u. It is found that increase in Ln retards the flow rapidly. The Fig.11 and Fig.12 illustrate the changes in velocity (v) with dimensionless numbers. Fig.11 displays the variation of v with the magnetic field (M). The velocity is found maximum in the mid region and further it is observed that the Lorentz force retard the velocity throughout the channel. Fig.12 demonstrate the changes of v with the Maxwell parameter (γ). The significance

144

of Maxwell fluid is clear in this figure and it is clearly noticed that the Maxwell fluid increases the velocity 'v'.

The Fig.13 to Fig.18 illustrate the changes in temperature (θ) with dimensionless numbers. The temperature falls gradually from left wall to right wall for all variations. Fig.13 illustrate the changes in temperature (θ) with magnetic field parameter (M). As the M increases temperature increases. Fig.14 illustrate the changes in temperature with Maxwell parameter (γ). The temperature enhances with increase in γ. This pronounces the Importance of Maxwell fluid in heating systems. Fig.15 illustrate the changes in temperature with thermal slip parameter (β). The temperature enhances significantly with β. This pronounces the Importance of thermal slip in heating systems. Fig.16 illustrate the changes in temperature with wave frequency (λ). The temperature enhances slightly with increase in λ. Fig.17 illustrate the changes in temperature with Brownian motion (Nb). The temperature linearly enhances slightly with increase in Brownian motion. Fig. 18 illustrate the changes in temperature with thermophoresis parameter (Nt). Increase in temperature observed with increase in Nt slightly. The Fig.19 to Fig.25 illustrate the changes in diffusion (S) with all dimensionless numbers. The diffusion linearly falls from left wall to right wall for all variations. Fig.19 depicts the changes of diffusion (S) with magnetic field parameter (M). As the M increases diffusion increases this signifies the domination of Lorentz force. Fig. 20 depicts the changes of diffusion with Maxwell parameter (γ). The diffusion enhances with increase in γ. This signifies the Importance of Maxwell fluid in heating systems. Fig.21 illustrate the changes in diffusion with molicular slip parameter (δ). The diffusion enhances with δ significantly showing its importance. Fig. 22 illustrate the changes in diffusion with wave frequency (λ). The diffusion enhances slightly with increase in λ. Fig. 23 displays the variation of diffusion with thermophoresis parameter (Nt). Increase in diffusion observed with increase in Nt slightly. Fig. 24 illustrate the changes in diffusion with Ln. The diffusion enhances significantly with the enhancement of Ln in the mid region of the channel particularly. Fig. 25 depicts the changes of diffusion with Brownian motion parameter (Nb). The diffusion enhances with increase in Brownian motion.

The rate of heat transfer (Nusselt Number, Nu-1) on the left wavy wall (or source) is tabulated in Table -1 for various dimensionless numbers. The heat transfer rate is notablly down-trodden for increase in both Grashof numbers Gr and Gc. The buoyancy force enhances the flow so that the rate of heat transfer reduces gradually. The thermal slip reduces the heat transfer rate significantly, hence can be used in cooling systems. The Maxwell parameter, thermophoresis parameter and Brownian motion parameter rapidly increase the heat transfer's rate. The transfer of heat is delayed by the wave frequency.

The Heat Transfer's rate (Nusselt Number, Nu-2) on the right wavy wall is tabulated in Table -2 for various dimensionless numbers. The Heat Transfer's rate is sgnificantly increases for increase in both Grashof numbers Gr and Gc. The thermal slip increases The Heat Transfer's rate significantly, The Maxwell parameter and Brownian motion parameter enhances The Heat Transfer's rate, on the other hand, thermophoresis parameter retards the rate of heat transfer notably. The wave frequency retards the Heat Transfer's rate.

The Heat Transfer's rate (Sherwood Number, Sh-1) on the left wavy wall is tabulated in Table -3 for various dimensionless numbers. The rate at which mass is transferred is notably retards for

145

increase in both Grashof numbers Gr and Gc. So the buoyancy force is dominated by viscous force in mass transfer. The diffusion slip retards the mass transfer rate, The Maxwell parameter and Thermophoresis parameter retards, the rate at which mass is transferred on the other hand Brownian motion parameter increases the mass transfer's rate notably . The wave frequency retards the rate at which mass is transferred slightly. The Lorentz force enhances the mass transfer rate. The rate of mass transfer (Sherwood Number, Sh-2) on the right wavy wall is tabulated in Table -4 for various dimensionless numbers. The mass transfer retards with increase in Lorentz force. The mass transfer rate significantly enhances for increase in both Grashof numbers Gr and Gc. So the buoyancy force is dominates the viscous force in mass transfer. The diffusion slip retards the rate at which mass is transferred significantly. The Maxwell parameter, Thermophoresis parameter and the Brownian motion parameter increases the mass transfer's rate significantly. The wave frequency retards mass transfer rate slightly. Ln retards the mass transfer rate significantly.

Table – 1. Nusselt Number (Nu-1) Values on the left wall (Source Wall)

γ	δ	β	Nb	Nt	Gr	Ln	λ	Gc	M	$Nu\text{-}1$
0.5	0.5	0.5	0.8	0.8	5	0.8	0.5	5	0.5	−0.35095726568190777
0.1										−0.35210248998939153
0.8										−0.353298051728984
	0.1									−0.3467131681111124
	0.8									−0.3541344812549946
		0.1								−0.7010062863680351
		0.3								−0.4571641979410439
		0.8								−0.23159959319369267
			0.5							−0.34549141508804815
			1.0							−0.34978700228370624
				0.5						−0.3236116189766508
				1.0						−0.35098258571070406
					2					−0.36149786185610555
					8					−0.335401522127231
					10					−0.28251709160795657
						0.5				−0.33397763180432477
						1.0				−0.3572314396216127
						1.2				−0.3615401264601923
							0.1			−0.35095726568255337
							0.3			−0.3509572656823364
							0.8			−0.3509572656808894
								2		−0.37102060965082806
								8		−0.28147041148755153
								10		−0.28010098319550397
									0.1	−0.34740160952630544
									0.3	−0.34926318667456224
									0.8	−0.3532170638948285

Table – 2. Nusselt Number (Nu-2) Values on the right wall

γ	δ	β	Nb	Nt	Gr	Ln	λ	Gc	M	$Nu\text{-}2$
0.5	0.5	0.5	0.8	0.8	5	0.8	0.5	5	0.5	−0.5094174471263075

γ	δ	β	Nb	Nt	Gr	Ln	λ	Gc	M	
0.1										−0.49384560033812636
0.8										−0.535857057487771
1.0										−0.5517436459640489
	0.1									−0.5164894779252788
	0.8									−0.5042401287806896
	1.2									−0.4974976376053277
		0.1								−0.482294960485521
		0.3								−0.4973138887009377
		0.8								−0.5968465272235898
			0.5							−0.5150534791175659
			1.0							−0.5206643701410184
			1.2							−0.5375773204775938
				0.5						−0.5874660336158946
				1.0						−0.4749292744760543
				1.2						−0.451078212899392
					2					−0.4426064241409546
					8					−0.6367600851666839
					10					−0.7361240765014635
						0.5				−0.5788941421055873
						1.0				−0.48968679624377853
						1.2				−0.477712027564287
							0.1			−0.5094174471326712
							0.3			−0.5094174471305324
							0.8			−0.5094174471163083
								2		−0.42114349739679613
								8		−0.7350418396741405
								10		−0.7257944223686424
									0.1	−0.5303104642916306
									0.3	−0.5191112577717178
									0.8	−0.49695527414537516

Table – 3. Sherwood Number (Sh-1) Values on the left wall

γ	δ	β	Nb	Nt	Gr	Ln	λ	Gc	M	Sh-1
0.5	0.5	0.5	0.8	0.8	5	0.8	0.5	5	0.5	−0.1777250947278825
0.1										−0.1882594057916728
0.8										−0.16222642932342396
1.0										−0.1496436267537005
	0.1									−0.1809696769008771
	0.8									−0.17504958223551742
	1.2									−0.1711627648818501
		0.1								−0.17004902521933304
		0.3								−0.18926443787736252
		0.8								−0.10780894456570937
			0.5							−0.010252872686247298
			1.0							−0.23617906908393332
			1.2							−0.2720675544934054
				0.5						−0.20498173045500756
				1.0						−0.1513172540112733
				1.2						−0.12984557824478438

γ	δ	β	Nb	Nt	Gr	Ln	λ	Gc	M	
					2					−0.230338267522719
					8					−0.10871417720031916
					10					−0.07665221194155354
						0.5				−0.02367382655306866
						1.0				−0.22819738509559837
						1.2				−0.2592269727890732
							0.1			−0.17772509472542608
							0.3			−0.17772509472625214
							0.8			−0.17772509473173756
								2		−0.25351349470726176
								8		−0.07439235531890534
								10		−0.07828331461953322
									0.1	−0.16411752404042898
									0.3	−0.17126373780617657
									0.8	−0.18641722275869024

Table – 4. Sherwood Number (Sh-2) Values on the right wall

γ	δ	β	Nb	Nt	Gr	Ln	λ	Gc	M	*Sh-2*
0.5	0.5	0.5	0.8	0.8	5	0.8	0.5	5	0.5	−0.7010062863889682
0.1										−0.6821212154680909
0.8										−0.7293005964501594
1.0										−0.7468135359983925
	0.1									−0.7266795101018935
	0.8									−0.6821616157181637
	1.2									−0.6575599237020081
		0.1								−0.17004902521933304
		0.3								−0.6121221489845894
		0.8								−0.9245014202323881
			0.5							−1.1474509919566072
			1.0							−0.5836694607331177
			1.2							−0.5150072758029778
				0.5						−0.6867241007894088
				1.0						−0.7606748623071188
				1.2						−0.8590400488819613
					2					−0.6147535979569465
					8					−0.835368165243811
					10					−0.9015875320265009
						0.5				−1.0215793771679682
						1.0				−0.6158213390154288
						1.2				−0.5653872155918542
							0.1			−0.7010062864022799
							0.3			−0.7010062863978063
							0.8			−0.7010062863680351
								2		−0.5821441179256668
								8		−0.9588459313055422
								10		−0.8084513440674316
									0.1	−0.7273169817659604
									0.3	−0.7133421278050761
									0.8	−0.6848477330882148

5. Conclusions:

1. The maximum flow is located in the middle region of the channel for all variations. Both velocities (u, v) vary rapidly with thermal slip and slightly with diffusion slip.

2. Temperature gradually decreases across the channel for all variations of dimensionless numbers from source to sink. The temperature enhances notably with Maxwell fluid parameter and thermal slip and molecular slip parameters.

3. The diffusion linearly decreases from left to right in the channel. Diffusion notably enhances with Ln and the diffusion slip parameters.

4. The thermal slip retards the rate of heat transfer significantly on the source wall but enhances on the right wall. The Maxwell parameter enhances the heat transfer rate on both walls notably.

5. The Mass transfer rate significantly enhances with slip parameter where as the wave frequency affects the mass transfer slightly. Buoyancy force affects the mass transfer rate on both walls significantly.

6. ACKNOWLEDGEMENTS:

7. References:

1. L.Y. Zhang, R.J. Duan,Y. Che, Z. Lu, X. Cui, L.C. Wei, L.W. Jin. A numerical analysis of fluid flow and heat transfer in wavy and curved wavy channels, *International Journal of Thermal Sciences*.2022;171:107248, https://doi.org/10.1016/j.ijthermalsci.2021.107248.

2. Igor V. Miroshnichenko , Mikhail A. Sheremet , Ioan Pop , Anuar Ishak. Convective heat transfer of micropolar fluid in a horizontal wavy channel under the local heating, *International Journal of Mechanical Sciences*.2017;128-129:541-549, https://doi.org:10.1016/j.ijmecsci.2017.05.013.

3. Abdullah Dewar, Zahir Shah, Muhammad Idress, Waris khan, Saeed Islam and Taza Gul. Impact of Thermal Radiation and Heat source /sink on Eyring – powell fluid over an unseady Oscillatory porous Stretching Surface, *Mathematical and Computational Applications*, 2018; 23(2): 20, https://doi.org:10.3390/mca23020020.

4. S.E. Ghasemi, Sina Gouran, Ali Zolfagharian. Hydrodynamic analysis of a conducting nanofluid flow through a sinusoidal wavy channel, *Case* Thermal and *Studies in Thermal Engineering*,2021;28:101642, https://doi.org:10.1016/j.csite.2021.101642.

5. Waqas Hassan, Shan Ali Khan, Sami Ullah Khan, M. Ijaz Khan, Seifedine Kadry, Yu-Ming Chu. Falkner-Skan time-dependent bioconvrction flow of cross nanofluid with nonlinear

149

thermal radiation, activation energy and melting process, *International Communication in Heat Mass Tran.*, 2021;20:105028. https://doi.org:10.1016/j.icheatmasstransfer.2020.105028.

6. Mehwish Manzur, Masood ur Rahman, Masood Khan. Computational study of Falkner–Skan flow of chemically reactive Cross nanofluid with heat generation/absorption, *Physica A:Statistical Mechanics and its Applications*, 2020;554:24267. https://doi.org:10.1016/j.physa.2020.124267.

7. S.E. Ghasemi, A.A. Ranjbar, M.J. Hoseini. Forced convective heat transfer of nanofluid as a coolant flowing through a heat sink: experimental and numerical study, *Journal of Molecular Liquids*, 2017; 248:264–270. https://doi.org:10.1016/j.molliq.2017.10.062.

8. Umair Khan, Anum Shafiq, A. Zaib, Abderrahim Wakif, Baleanu Dumitru. Numerical exploration of MHD falkner-skan-sutterby nanofluid flow by utilizing an advanced non-homogeneous two-phase nanofluid model and non-fourier heat-flux theory, *Alexandria Engineering Journal*, 2020;59(6):4851–4864. https://doi.org:10.1016/j.aej.2020.08.048.

9. Shafiq Ahmad, Sohail Nadeem, Noor Muhammad, Alibek Issakhov. Radiative SWCNT and MWCNT nanofluid flow of Falkner–Skan problem with double stratification, *Physica A:Statistical Mechanics and its Applications*, 2020;547:124054. https://doi.org:10.1016/j.physa.2019.124054.

10. S.E. Ghasemi, M. Hatami. Solar radiation effects on MHD stagnation point flow and heat transfer of a nanofluid over a stretching sheet, *Case Studies in Thermal Engineering*,2021;25:100898, https://doi.org:10.1016/j.csite.2021.100898.

11. Nadeem, S., Akhtar, S. and Abbas, N. Heat transfer of Maxwell base fluid flow of nanomaterial with MHD over a vertical moving surface. *Alexandria Engineering Journal*, 2020;59(3):1847-1856, https://doi.org:10.1016/j.aej.2020.05.008.

12. Hussain.A, Sarwar.L, Nadeem.S, Akbar.S, Jamal.S**.** Inquisition of combined effects of radiation and MHD on Elastico-viscous fluid flow past a pervious plate, *Journal of the Brazilian Society of Mechanical Sciences and Engineering*, 2018;40(7):343, https://doi.org/10.1007/s40430-018-1228-z .

13. Khan.Z, Haroon Ur Rasheed, T. A. Alkanha, M.Ullah, Ilyas Khan, I**.**Tlili. Effect of magnetic field and heat source on Upper-Convected-Maxwell fluid in a porous channel, *Open Physics*, 2018;16*:*917-928, https://doi.org:10.1515/phys-2018-0113 .

150

14. Sravanthi, C. S. and Gorla, R. S**.** Effects of heat source/sink and chemical reaction on MHD Maxwell nanofluid flow over a convectively heated exponentially stretching sheet using homotopy analysis method, *International Journal of Applied Mechanics and Engineering*, 2018;23(1):137-159, https://doi.org/10.1515/ijame-2018-0009.

15. Farooq, U., Lu, D., Munir, S., Ramzan, M., Suleman, M. and Hussain, S**.** MHD flow of Maxwell fluid with nanomaterials due to an exponentially stretching surface, *Scientific Reports*, 2019; 9(1):732, https://doi.org/10.1038/s41598-019-43549-0.

16. Imran, M. A., Riaz, M. B., Shah, N. A. and Zafar, A. A**.** Boundary layer flow of MHD generalized Maxwell fluid over an exponentially accelerated infinite vertical surface with slip and Newtonian heating at the boundary, *Results in Physics*, 2018;8:1061-1067, https://doi.org/10.1016/j.rinp.2018.01.036

17. Veera Krishna, M. and Chamkha, A. J. Hall and ion slip effects on MHD rotating boundary layer flow of nano-fluid past an infinite vertical plate embedded in a porous medium, *Results in Physics*, 2019;15:02652, https://doi.org/10.1016/j.rinp.2019.102652.

18. Veera Krishna, M. and Chamkha, A. J. Hall effects on MHD Squeezing flow of a water based nano fluid between two parallel disks, *Journal of Porous Media*, 2019;22(2):209-223, https://doi**.**org/10.1615/JPorMedia.2018028721.

19. Krishna, M.V., Chamkha, A.J. Hall and ion slip effects on Unsteady MHD Convective Rotating flow of Nanofluids, Application in Biomedical Engineering, *Journal of the Egyptian Mathematical Society*,2020;28(1):2938, https://doi.org/0.86/s42787-09-0065-2.

20. Veera Krishna, M., Subba Reddy, G. and Chamkha, A. J**.** Hall effects on unsteady MHD oscillatory free convective flow of second grade fluid through porous medium between two vertical plates*, Physics of Fluids*, 2018;30(2):023106*,* https://doi.org/10.1063/1.5010863.

21. Veera Krishna, M. and Chamkha, A. J.. Hall effects on unsteady MHD flow of second grade fluid through porous medium with ramped wall temperature and ramped surface concentration, *Physics of Fluids*, 2018; 30(5):053101, https://doi.org/10.1063/1.5025542.

22. Veera Krishna, M., Jyothi, K. and Chamkha, A. J**..** Heat and mass transfer on MHD flow of second-grade fluid through porous medium over a semi-infinite vertical stretching sheet, *Journal of Porous Media*, 2020; 23(8):751-765, https://doi:10.1615/JPorMedia.202002387.

23. M. Veera Krishna, K. Bharathi and Ali J. Chamkha. Hall Effects On MHD Peristaltic Flow Of Jeffrey Fluid Through Porous Medium In A Vertical Stratum, *Interfacial Phenomena and*

Heat *Transfer*, 2018;6(3):253-268, https://doi:10.1615/InterfacPhenomHeatTransfer.2019030215.

24. Veera Krishna, M., Swarnalathamma, B. V. and Chamkha, A. J**..** Heat and mass transfer on magnetohydrodynamic chemically reacting flow of micropolar fluid through a porous medium with Hall effects, *Special Topics & Reviews in Porous Media: An International Journal*,2018;9(4):347-364, https://doi:10.1615/SpecialTopicsRevPorousMedia.2018024579.

25. Veera Krishna, M. and Chamkha, A. J**..** MHD Peristaltic Rotating Flow of a Couple Stress Fluid through a Porous Medium with Wall and Slip effects, *Special Topics & Reviews in Porous Media: An International Journal*, 2019;10(3):245-258, https://doi:10.1615/SpecialTopicsRevPorousMedia.2019028609.

26. Veera Krishna, M., Anand, P. V. S. and Chamkha, A. J**..** Heat and mass transfer on Free convective flow of a micropolar fluid through a porous surface with inclined magnetic field and Hall effects*, Special Topics & Reviews in Porous Media: An International Journal*, 2019; 10(3): 203-223, https://doi:10.1615/SpecialTopicsRevPorousMedia.2018026943.

27. Veera Krishna, M. and Chamkha, A. J**..** Hall and ion slip effects on MHD rotating flow of elastico-viscous fluid through porous medium, *International Communications in Heat and Mass Transfer*,2020;113:04494, https://doi.org/10.1016/j.icheatmasstransfer.2020.104494.

28. Mukhtar, T., Jamshed, W., Aziz, A., and Al-Kouz, W.. Computational investigation   of heat transfer in a flow subjected to magnetohydrodynamic of Maxwell nanofluid over a stretched flat sheet with thermal radiation, *Numerical Methods for Partial Differential Equations*, 2020: 22643, https://doi.org/10.1002/num.22643.

29. Sohail, M., Nazir, U., Chu, Y. M., Alrabaiah, H., Al-Kouz, W. and Thounthong, P**..** Computational exploration for radiative flow of Sutter by nanofluid with variable temperature-dependent thermal conductivity and diffusion coefficient, *Open Physics*, 2020; 18(1): 1073-1083, https://doi.org/10.1515/phys-2020-0216.

30. P.Venkataramana, S.V. Ranganayakulu, G. Srinivas. Heat Transfer Through Nano Fluid in a Vertical Wavy Channel with Travelling Thermal Waves, *International Journal of Mathematics Trends and Technology (IJMTT)*, 2018, 56(6):455-462, https://ijmttjournal.org/archive/ijmtt-v56p560